

A NOVEL ELECTRICAL TOMOGRAPHY SENSOR FOR MONITORING THE PHASE DISTRIBUTION IN INDUSTRIAL REACTORS

G.T. Bolton, C.H. Qiu and M. Wang*

Industrial Tomography Systems, 47 Newton Street, Manchester, M1 1FT.

*School of Process, Environmental and Materials Engineering, University of Leeds, Leeds, LS2 9JT, UK

A linear sensor array has been developed based on the measurement technique Electrical Resistance Tomography (ERT) for measuring the phase distribution within multi-phase processes. The electric field generated by the sensor, comprising a linear row of multiple electrodes, penetrates the process volume both radially and axially thus providing information in both these planes. Numerical analysis of the electric field intensity was performed to optimise sensor design. The sensor has been scaled up from a laboratory prototype to form an integral part of a glass-lined steel baffle for applications in chemically hostile environments. Tomographic images showing the distribution of solids in a liquid are presented. Further data processing of the images generates axial solid distribution plots.

Keywords: mixing, electrical, tomography, reactor, phase, distribution,

INTRODUCTION

Electrical Process Tomography measurement techniques are becoming established research tools for providing spatial information on the phase distribution and flow patterns of multiphase chemical processes as detailed in a recent review by York¹. This is particularly true of Electrical Capacitance Tomography (ECT) and Electrical Resistance Tomography (ERT) measurement techniques which are available as commercial systems. Of these techniques, ERT is most suited to the study of mixing processes due to the availability of multi-plane measurement systems and the scalability of ERT sensors. The maturity of this applied research field can be judged by the wealth of references from throughout the 90s to recent years. Examples of the application of ERT to mixing processes spanning this period include Dickin *et al.*², Holden *et al.*³ and Cooke *et al.*⁴. In the majority of the reported studies, ERT is used to interrogate multiple layers through the stirred vessel by the use of a multi-plane sensor. Each sensor plane delivers a cross-section map of the electrical conductivity within the sensor plane. It is common to display the results as 3D solid body reconstructions interpolated from the multiple sensor planes as demonstrated by Holden *et al.*³. Studies have shown that ERT can be applied across a wide range of vessel scales from laboratory-scale to a stirred vessel of 1.43m diameter³. The information obtained has proven to be valuable and has attracted significant industrial interest as a research and development tool as demonstrated by Cooke *et al.*⁴. However this degree of information is likely to be superfluous in an operations environment. In addition the practicability of fitting an industrial reactor with up to 128 electrodes is likely to preclude this as an option.

With this in mind an electrical tomography linear sensor has been developed which delivers the spatial information that is the main benefit of tomographic measurement techniques whilst being suitable for installation in industrial reactors. The main process output of the sensor was to be a measurement of axial mixing as inadequate axial mixing is a cause of many industrial mixing problems. It should be emphasised that since the measurement technique is electrical it offers the usual benefits of such techniques as described by Richardson and Holdich⁵:

- The measuring circuit is relatively simple
- Measurements can be easily automated at regular intervals or be continuous
- Low currents result in a safe technique
- Providing there is significant contrast in the conductivity of the phases, measurements can be made over a wide range of concentrations

The probe has been designed to operate with a commercial P2000 ERT system by Industrial Tomography Systems. This system is a direct development of the ERT systems designed at UMIST throughout the 1990s, for example see Dickin and Wang⁶. The use of the P2000 for investigating a diverse range of chemical processes including hydrocyclones (Williams *et al.*⁷), bubble column reactors, (Wang *et al.*⁸) and stirred tanks (Mann *et al.*⁹) is well reported in the literature. An advantage that is often cited of traditional circular electrical tomography sensors is their non-invasive nature. The linear ERT probe may still meet this criterion by placing electrodes next to the vessel wall. However, it will be seen in a later section that one of the long term aims of this development is to incorporate the sensor within existing off the wall baffles resulting in an invasive measurement technique. In this case no additional reactor internals are required since the sensor is integral to the baffle.

SENSOR DESIGN

The principles of the sensor developed during this study are based upon a linear ERT sensor first reported by Qiu *et al.*¹⁰ for laboratory experiments simulating the seabed environment. In brief, the adjacent measurement strategy (Brown and Segar¹¹) is applied to the linear ERT sensor. A constant amplitude current is injected between the top and the bottom electrodes on the sensor and the resultant voltage differences are measured between neighbouring electrode pairs not participating in current injection. The same current amplitude is then injected between the first pair of neighbouring electrodes (e.g. 1&2) and the resulting voltage differences measured between all other pairs of neighbouring electrodes. This latter procedure is repeated for all measurement combinations. For n electrodes there are $n(n-3)/2$ independent measurements. A qualitative tomographic image is reconstructed from these measurements using a sensitivity coefficient back projection algorithm to delineate the change in conductivity from a previously acquired 'homogeneous' situation.

SENSOR SIMULATION

Numerical analysis of the electric field was performed using commercially available software (Ansoft's Maxwell 3D Field Simulator). Figure 1 shows an example of a vessel and probe geometry on which numerical analysis of the electric field intensity was performed. The height and diameter of the vessel were both set to 100 mm. The probe is located midway along a radius at x, y coordinates of 25, 0. The red objects along the length of the measurement probe represent the electrodes which are 3 mm by 3 mm with inter-electrode spacing of 7 mm. Figures 2, 3 and 4 show the results obtained for this particular geometry when electrodes 4 and 5 are excited. Figure 2 shows the electric field intensity contours in the x - y plane at $z = 45$ (between electrodes 4 and 5) and figure 3 shows the electric field intensity contours in the y - z plane at $x = 0$. Figure 4 shows the magnitude of electric field intensity along a diameter passing through the centre of the vessel and the probe at $z = 45$. This simulation provides a powerful tool for optimisation of the sensor geometry.

Figure 1. Vessel and probe geometry for simulation.

Figure 2. Electric field intensity in x-y plane at $z = 45$.

Figure 3. Electric field intensity in y-z plane at $x = 0$.

Figure 4. Electric field intensity along a diameter through the vessel centre and probe at $z = 45$.

LABORATORY-SCALE PROBE

Figure 5 shows a sensor which was designed and manufactured for laboratory mixing studies. The main structure of the sensor was a PTFE cylinder of length 350 mm and outside diameter 30 mm. Sixteen ring-electrodes of height 4 mm were fitted uniformly along the cylinder with an inter-electrode gap of 10 mm. Cables from each electrode pass through the centre and exit at the top of the cylinder. The cables terminate in an IEEE-488 centronics plug which interfaces with the P2000 data acquisition system. The use of ring-electrodes results in the electric field interrogating the entire 360° around the sensor axis. The sensing region can be concentrated within a certain part of the process volume by covering part of the electrodes.

Figure 5. Laboratory-scale probe.

PILOT PLANT PROBE

The internal surfaces of reactors used in chemically corrosive and hostile environments are commonly lined with glass which is extremely resistance to corrosion and mechanical stress. Using traditional glass lining techniques it is only possible to line one surface of a piece of steel and it is difficult to apply glass to sharp edges. Consequently glass-lined reactors do not normally employ traditional sidewall baffles as found on stainless steel and hastelloy reactors. Rather, the baffles are in the form of cylindrical tubes which pass through the reactor lid and immerse in the process fluids. Due to the competition for ports on the reactor lid it is common to use only one baffle. In addition agitator types are limited to those that can be lined with glass such as the Retreat Curve Impeller (RCI). Overall, the mixing in such reactors can be inefficient compared to stainless steel and hastelloy reactors.

A linear ERT sensor integral to a glass lined steel baffle fabricated by Pfaudler-Balfour to fit the AE630 pilot reactor at their Research and Development facilities is shown in Figure 6. The sensor had a length and diameter of 1200 mm and 120 mm respectively and was fitted with 10 platinum electrodes.

Figure 6. Glass-lined sensor for AE630 pilot reactor.

EXPERIMENTAL

LABORATORY TESTS

The sensor was placed in a simple laboratory stirred tank consisting of a cylindrical vessel with four sidewall baffles and a six pitched-blade agitator with variable speed drive as shown in Figure 7. The stirred tank had an operating capacity of approximately 50 litres. The sensor had a clearance equivalent to 10% of the tank diameter from the wall mid-way between two of the baffles. Prior to placing the sensor in the vessel the electrodes had 50% of their surface

area covered. The uncovered electrode area for measurement purposes was directed into the central region of the vessel with the covered electrode area facing the vessel wall.

The vessel was filled with water to an operating level of 400 mm. Solids were added to give an overall solids concentration of 3% w/w. The agitator was switched on and the speed was incrementally increased until the solids appeared well distributed.

Figure 7. Laboratory mixing facility.

PILOT PLANT TESTS

The Pfaudler-Balfour R&D vessel is an AE630 type with an internal diameter of 1000 mm and a maximum capacity of 865 litres. Figure 8 shows a photograph of the reactor with the sensor contained within the port in the centre of the photograph. The reactor was filled to an operating level of 700 mm above the tan line giving an approximate operating volume of 630 litres. Figure 9 shows a photograph of the sensor located within the reactor.

The agitator speed was set to 40 rpm, a reference measurement was taken under these conditions and measurements were started. After a short period of time 5 kg of plastic chips were added to the vessel through the viewing port. The reactor was allowed to reach steady-state conditions and a further 5 kg of solids were added. This was repeated three times until there was 25 kg of solids in the reactor representing a solids content of 4% w/v.

A second experiment was performed with 25 kg of plastic chips in the reactor. A reference frame was taken under conditions of no agitation and measurements were started. The agitator speed was increased in small steps up to a maximum of 100 rpm.

Figure 8. Photograph of AE630 pilot plant reactor.

Figure 9. Photograph of sensor located within reactor.

RESULTS

LABORATORY TESTS

Figure 10 shows the tomographic images collected before and after the addition of solids to the vessel. A blue-green-red colour scale is used to represent the conductivity range. Red corresponds to the background water conductivity (zero solids concentration) with blue indicating low conductivity (and hence high solids concentration). Figure 10(a) shows the background measurement before the addition of solids. As expected the distribution of electrical conductivity is uniform reflecting the presence of a single material within the sensing volume. Figure 10(b) shows the addition of solids to the vessel clearly detected by the blue shading at the bottom of the image. As the agitation is increased the deep blue colour is replaced by a green/ yellow colouring indicating that the solids have become well mixed within the sensing volume. Each image is an average of several images collected when the contents of the reactor were at steady state. The data collection time for a single image is approximately 30 ms. The addition of solids and their distribution throughout the sensing volume as the agitation rate is increase is clearly detected.

Figure 10. Tomographic images of (a) before addition of solids and following the addition of solids at agitation rates of (b) 0, (c) 113, (d) 144, (e) 181, (f) 233, (g) 286 and (h) 343 rpm.

The tomographic image comprises 20 x 10 pixels gives electrical conductivity distribution information in both axial and radial directions. By averaging each row of pixels it is possible to determine the axial electrical conductivity distribution within the measurement volume. Solids concentration can be calculated from electrical conductivity data by applying a correlation such as the Maxwell equation (Lucas *et al.*¹²). Figure 11 shows the results of this procedure applied to the tomographic images from Figure 10.

Figure 11. Axial solids distribution for range of agitation rates.

PILOT PLANT TESTS

Figure 12 shows the tomographic images collected at an agitation rate of 40 rpm while solids were added to reactor in steps of 5 kg up to a total of 25 kg. In this case a blue-green colour scale is used to represent the conductivity range. The background water is represented by the green colour and deeper shades of blue correspond to lower conductivity and hence the presence of solids. The increase in the overall solids content is clearly shown by the increased regions of blue colouring on the images from Figure 12(b) through Figure 12(f).

Figure 12. Tomographic images at agitation rate of 40 rpm (a) before solids addition and (b)-(f) following the addition of 5kg batches of solids.

Figure 13 shows the tomographic images for the experiment conducted with 25 kg of solids in the reactor. Initially the agitator was switched off and then it was increased in small intervals to a maximum of 100 rpm. As agitation is started it can be seen that solids appear in the base of the vessel in Figure 13(d). By changing the image scale, smaller changes can be detected. Increasing the agitation rate above 35 rpm appears to have little effect on the distribution of the solids. The axial distribution of the solids derived from these images is shown in Figure 14.

Figure 13. Tomographic images for 25 kg of solids at agitation rates of (a) 0, (b) 10, (c) 15, (d) 20, (e) 25 (f) 30, (g) 35, (h) 40, (i) 45, (j) 60, (k) 80 and (l) 100 rpm.

Figure 14. Axial solids distribution in an industrial reactor at a range of agitation speeds.

CONCLUSIONS

The application of a linear electrical tomography sensor to laboratory and pilot-scale stirred vessels has demonstrated the measurement of solids concentration and distribution. This sensor is suitable for one-off trouble shooting and process optimisation studies of industrial process vessels. The sensor is also suitable for retrofitting to industrial process vessels for on-line measurement of phase distribution. By incorporating the sensor within a glass-lined baffle, valuable information on the phase distribution within industrial pharmaceutical reactors may be possible. The sensor is currently undergoing accreditation for use in potentially explosive atmospheres to allow application to industrial processes.

REFERENCES

1. York, T., 2001, Status of electrical tomography in industrial applications, *Journal of Electronic Imaging*, Vol. 10(3), 608-619

2. Dickin, F.J., Williams, R.A. and Beck, M.S., 1993, Determination of composition and motion of multicomponent mixtures in process vessels using electrical impedance tomography, *Chem Eng Sci*, 48(10), 1883-1897
3. Holden, P.J., Wang, M., Mann, R., Dickin, F.J. and Edwards, R.B., 1998, Imaging stirred-vessel macromixing using electrical resistance tomography, *AIChE J*, 44(4): 780-790
4. Cooke, M., Bolton, G.T., Jones, D.H. and Housley, D., 2001, Demonstration of a novel retrofit tomography baffle cage for gas-liquid mixing studies under intense operating conditions, *Proceedings of Second World Congress on Industrial Process Tomography*, 29-31 August, Hannover, Germany, ISBN 0 85316 224 7
5. Richardson, D.J, and Holdich, R.G., 2001, A novel and low cost probe for monitoring dispersed solids concentrations in liquids, *Trans IChemE*, 77(A), 709-712
6. Dickin, F.J. and Wang, M., 1996, Electrical resistance tomography for process applications, *Meas Sci Technol*, 7, 247-260
7. Williams, R.A., Jia, X., West, R.M., Wang, M., Cullivan, J.C., Bond, J., Faulks, I., Dyakowski, T., Wang, S.J., Climpson, N., Kostuch, J.A. and Payton, D., 1999, Industrial Monitoring of Hydrocyclone Operation using Electrical Resistance Tomography, *Minerals Engineering*, 12(10), 1245-1252
8. Wang, M., Jia, X., Bennet, M.A. and Williams, R.A., 2001, Flow regime identification and optimum interfacial area control of bubble columns using electrical impedance imaging, *Proceedings of Second World Congress on Industrial Process Tomography*, 29-31 August, Hannover, Germany, ISBN 0 85316 224 7
9. Mann, R., Dickin, F.J., Wang, M., Dyakowski, T., Williams, R.A., Edwards, R.B., Forrest, A.E. and Holden P.J., 1997, Application of Electrical Resistance Tomography to Interrogate Mixing Processes at Plant Scale, *Chem Eng Sci*, 52(13), 2087-2097
10. Qiu, C.H., Dickin, F.J. James, A.E. and Wang, M., 1994, Electrical resistance tomography for imaging sub-seabed sediment porosity: initial findings from laboratory-scale experiments using spherical glass beads, *Proc. of 3rd European Concerted Action on Process Tomography*, 24-26 March, Oporto, Portugal
11. Brown, B.H. and Segar, A.D., 1985, Applied potential tomography: data collection problems, *Proc. IEE Int. Conf. On Electric and Magnetic field in Medic. And Biolo.*, 79-82
12. Lucas, G.P., Cory, J., Waterfall, R.C., Loh, W.W., Dickin, F.J., 1999, Measurement of the solids volume fraction and velocity distributions in solids-liquid flows using dual-plane electrical resistance tomography, *Flow Measurement and Instrumentation*, 10, 249-258

ACKNOWLEDGEMENTS

The authors thank Pfaudler-Balfour Ltd., Leven, Fife for manufacturing the glass-lined baffle sensor and for use of the AE630 pilot plant reactor.

ADDRESS

Correspondence concerning this paper should be addressed to Dr G.T. Bolton, Industrial Tomography Systems Ltd, 47 Newton Street, Manchester, M1 1FT, UK. (E-mail: gary.bolton@itoms.com).

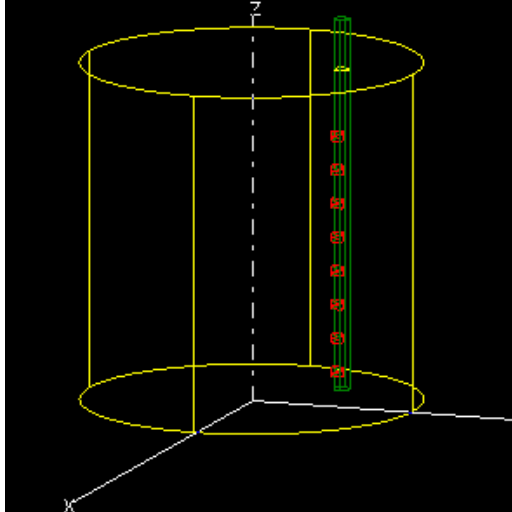


Figure 1. Vessel and probe geometry for simulation.

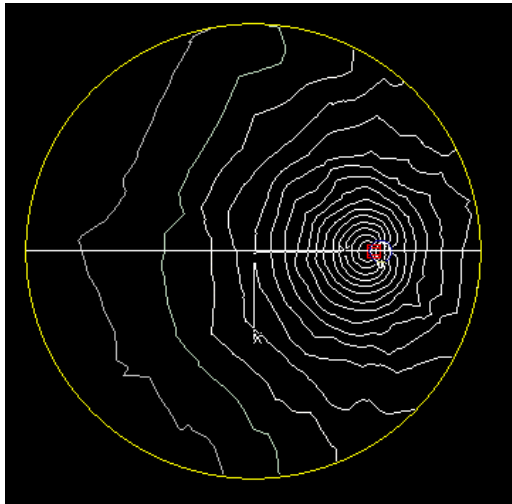


Figure 2. Electric field intensity in x-y plane at $z = 45$.



Figure 5. Laboratory-scale probe.

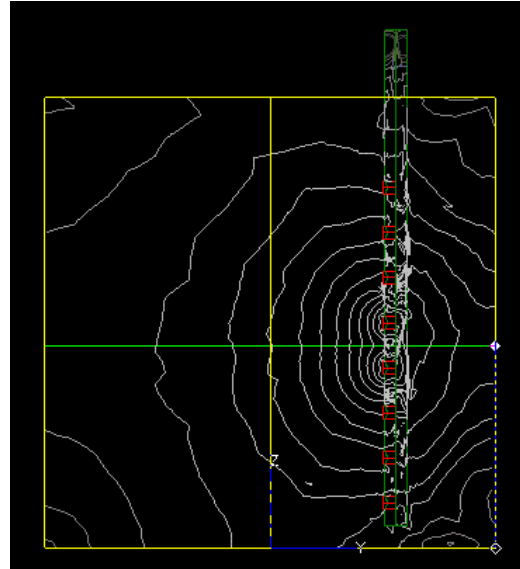


Figure 3. Electric field intensity in y-z plane at $x = 0$.

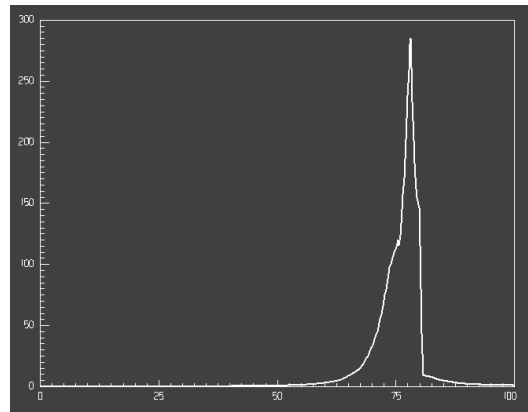


Figure 4. Electric field intensity along a diameter through the vessel centre and probe at $z = 45$.



Figure 6. Glass-lined sensor for AE630 pilot reactor.

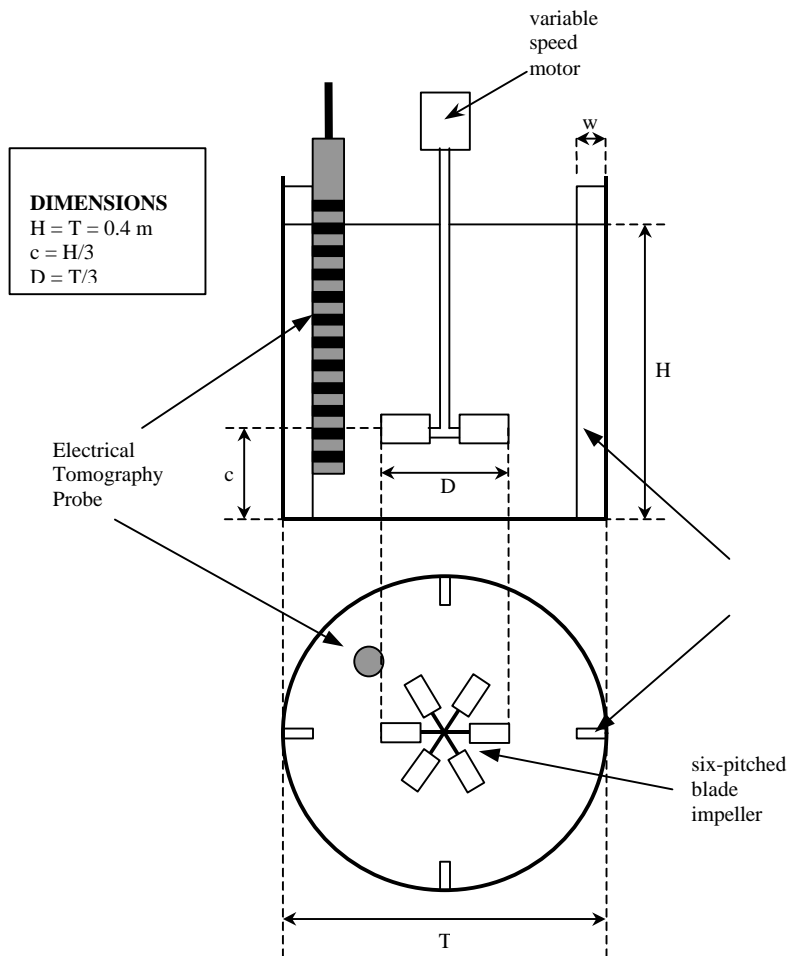


Figure 7. Laboratory mixing facility.



Figure 8. Photograph of AE630 pilot plant reactor.

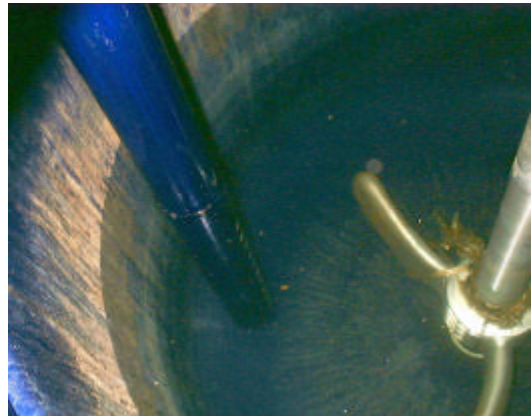


Figure 9. Photograph of sensor located within reactor.

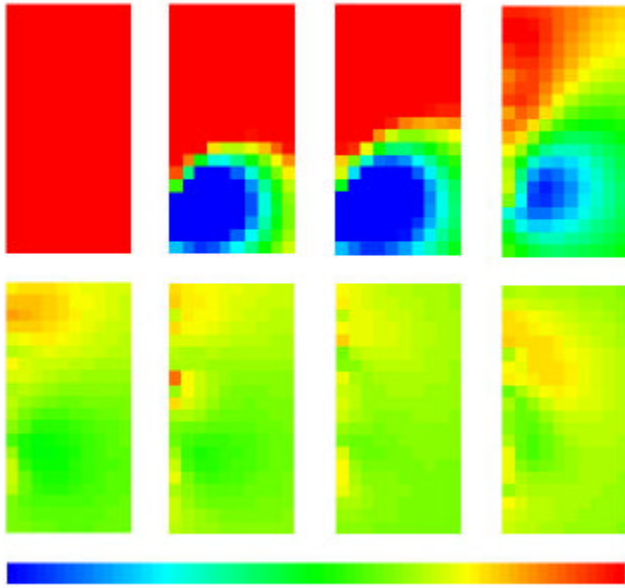


Figure 10. Tomographic images of (a) before addition of solids and following the addition of solids at agitation rates of (b) 0, (c) 113, (d) 144, (e) 181, (f) 233, (g) 286 and (h) 343 rpm.

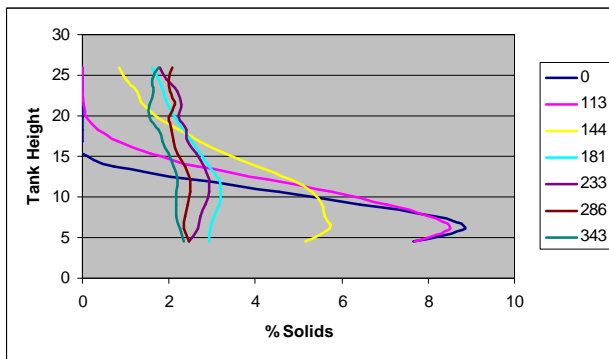


Figure 11 Axial solids distribution for range of agitation rates.

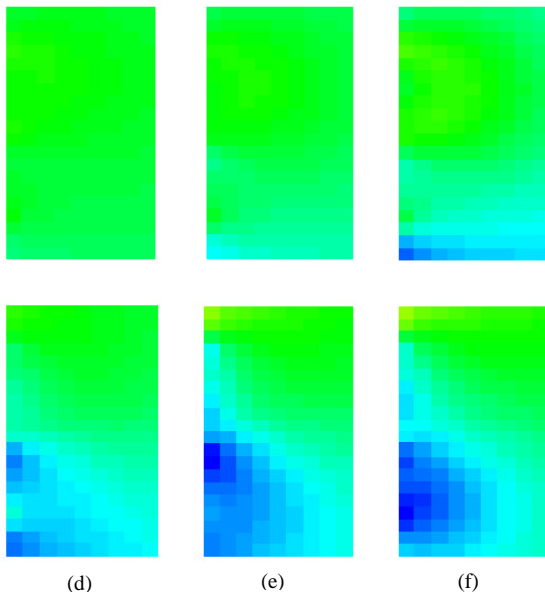


Figure 12. Tomographic images at agitation rate of 40 rpm (a) before solids addition and (b)-(f) following the addition of 5kg batches of solids.

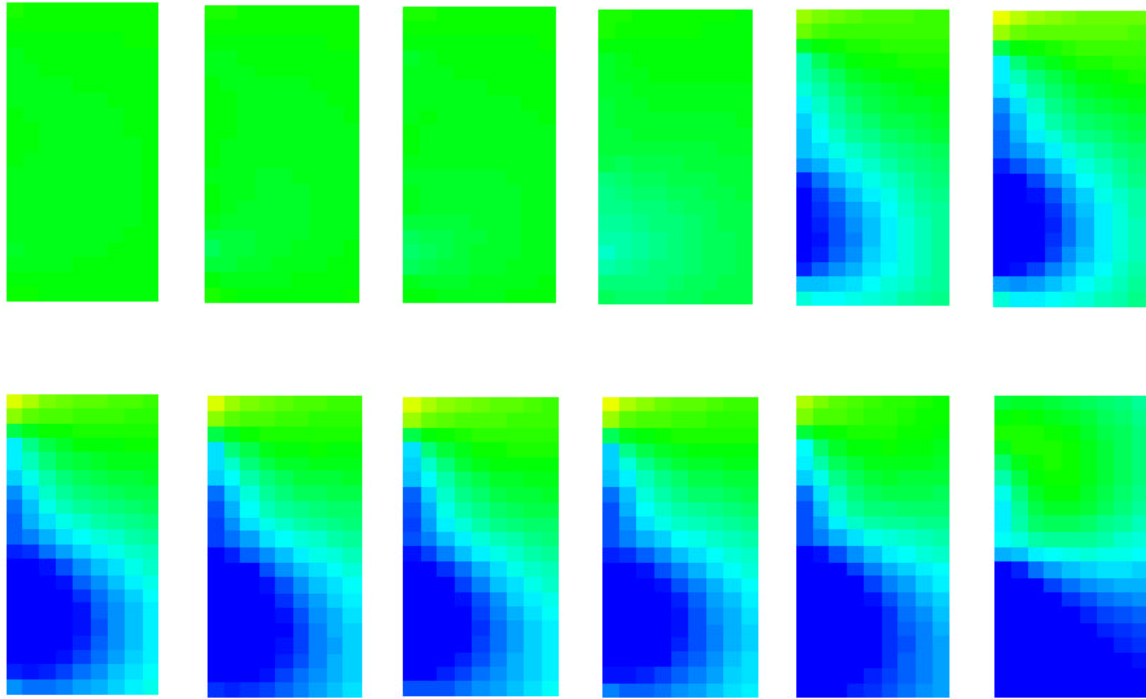


Figure 13. Tomographic images for 25 kg of solids at agitation rates of (a) 0, (b) 10, (c) 15, (d) 20, (e) 25 (f) 30, (g) 35, (h) 40, (i) 45, (j) 60, (k) 80 and (l) 100 rpm.

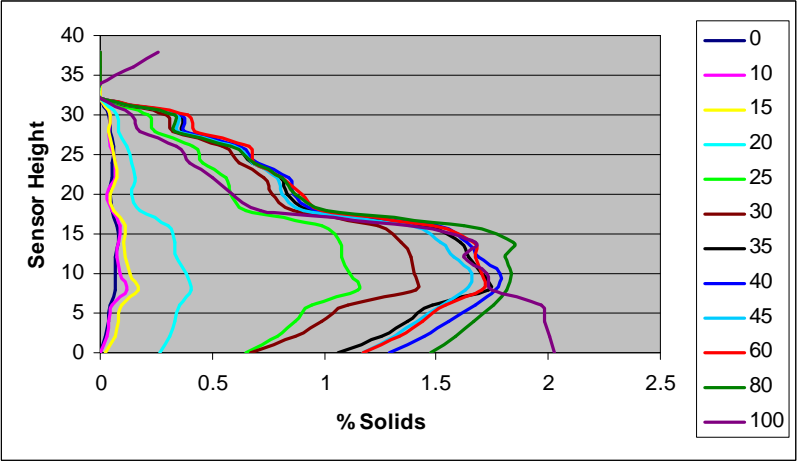


Figure 14. Axial solids distribution in an industrial reactor at a range of agitation speeds.